ACS OMEGA

http://pubs.acs.org/journal/acsodf

Article

Lipid Flip-Flop-Inducing Antimicrobial Phytochemicals from *Gymnema sylvestre* are Bacterial Membrane Permeability Enhancers

Himadri Gourav Behuria, Gandarvakottai Senthilkumar Arumugam, Chandan Kumar Pal, Ashis Kumar Jena, and Santosh Kumar Sahu*

Cite This: *ACS Omega* 2021, 6, 35667−35678

Read Online

ACCESS | Metrics & More | Article Recommendations

ABSTRACT: An amphiphilic phytochemical fraction isolated from methanol extract of *Gymnema sylvestre* leaf powder contained six terpenoids, two flavonoids, and one alkaloid that induced rapid flip-flop of fluorescent phospholipid analog in the phosphatidyl choline bilayer. Lipid-flipping activity of the methanol-extracted fraction of *G. sylvestre* (MEFGS) was dose-dependent and time-dependent with a rate constant k = (12.09 ± 0.94) mg^{-1} min^{-1} that was saturable at (40 ± 1) % flipping of the fluorescent lipid analogue. Interactions of MEFGS phytochemicals with large unilamelar vesicles led to time-dependent change in their rounded morphology into irregular shapes, indicating their membrane-destabilizing activity. MEFGS exhibited antibacterial activity on *Escherichia coli* (MTCC-118), *Staphylococcus aureus* (MTCC-212), and *Pseudomonas aeruginosa* (MTCC-1035) with IC_{50} values 0.5, 0.35, and 0.1 mg/mL, respectively. Phytochemicals in MEFGS increased membrane permeabilization in all three bacteria, as indicated by 23, 17, and 17% increase in the uptake of crystal violet, respectively. MEFGS enhanced membrane damage, resulting in a 3−5 fold increase in leakage of cytosolic ions, 0.5−2 fold increase in leakage of PO_4^-, and 15−20% increase in loss of cellular proteins. MEFGS synergistically increased the efficacy of curcumin, amoxillin, ampicillin, and cefotaxime on *S. aureus* probably by enhancing their permeability into the bacterium. For the first time, our study reveals that phytochemicals from *G. sylvestre* enhance the permeability of the bacterial plasma membrane by facilitating flip-flop of membrane lipids. Lipid-flipping phytochemicals from *G. sylvestre* can be used as adjuvant therapeutics to enhance the efficacy of antibacterials by increasing their bioavailability in the target bacteria.

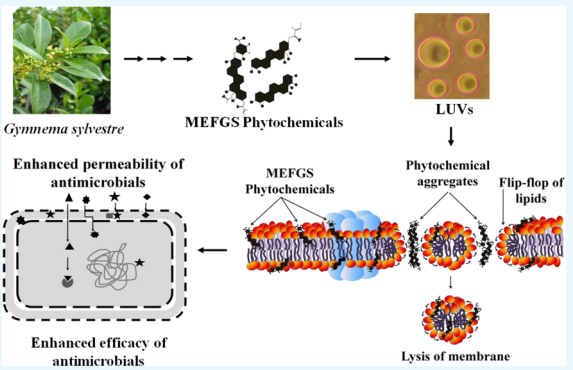

1. INTRODUCTION

Increasing resistance of human pathogenic bacteria to existing antimicrobials is a rapidly growing global health problem that instigates repeated discovery of more efficient drugs. However, limiting factors such as low pathogen specificity, high toxicity toward host cells, insolubility in aqueous body fluid, poor bioavailability in target pathogen, and multi-drug resistance are the key bottlenecks of novel drug formulation.[1] In bacteria, two important multi-drug resistance mechanisms are (i) membrane impermeability and (ii) increased efflux, leading to reduced drug bioavailability inside the target pathogen.[2] Hence, bacterial membrane permeability enhancers and efflux pump inhibitors are promising new generation drug candidates or adjuvant therapeutics.[3] Phytochemicals constitute a natural resource of structurally diverse compounds that are currently being proposed as herbal drugs because of their low toxicity and absence of deleterious side effects.[4] However, their poor solubility and low membrane permeability are two major drawbacks that hinder their drug formulation. While phytochemicals with higher hydrophobic indices exhibit limited solubility in aqueous body fluid, those with lower hydrophobic indices exhibit membrane impermeability, leading to their poor bioavailability in target pathogens. Hence, selective purification of amphiphilic phytochemicals with enhanced membrane permeability and high solubility in aqueous body fluid are the prerequisites for their efficient therapeutic applications.[5]

Gymnema sylvestre (Retz.) R.Br. ex Sm, an ethno-medicinal plant, widely distributed across Asia, Africa, and Australia is traditionally used as a herbal remedy for type II diabetes.[6] Its pharmacologically enriched phytochemical extract exhibits hypoglycemic, anti-cancer, anti-inflammatory, and antimicrobial activities.[7] Most of its antimicrobial properties originate

Received: October 7, 2021
Accepted: December 7, 2021
Published: December 16, 2021

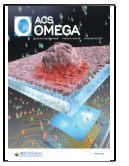

https://doi.org/10.1021/acsomega.1c05581
ACS Omega 2021, 6, 35667−35678

from the triterpenoid saponin "Gymnemic acid" and its derivatives, 53 different variants of which have been identified.[8] Terpenoids and flavonoids of *G. sylvestre* exhibit significant variability in their specificity and efficacy, indicating their differential antimicrobial mechanisms.[7] Although the membranotropic flavonoids exhibit their cytotoxicity by increasing rigidity of the bacterial plasma membrane, the mechanism of terpenoid action on bacteria remains elusive.[9] Terpenoids from *G. sylvestre* interact with the eukaryotic plasma membrane in a sterol-dependent manner, leading to their lysis.[10,11] However, their mechanism of interactions with the bacterial plasma membrane that exhibits significantly different lipid compositions needs to be investigated.

Amphiphilic terpenoids and flavonoids are potent membrane permeability enhancers that enhance the efficiency of antibiotics by increasing their bioavailability in target pathogens.[12] A recent investigation showed that antibacterial terpenoids from *G. sylvestre* induced rapid flip-flop of fluorescent phospholipid analogs in large unilamellar vesicles (LUVs).[13] Lipid flip-flop-inducing agents could perturb lipid organization, leading to their altered packing in the membrane, resulting in the increased permeability.[14] In this study, we identified the lipid flip-flop-inducing phytochemicals in the *G. sylvestre* leaf extract and investigated their effect on the bacterial membrane permeability.

2. RESULTS AND DISCUSSION

2.1. Purification and Characterization of Phytochemicals. Although it is cumbersome to purify a single plant compound, use of phytochemical fractions containing a group of compounds is more common because of their similar solubility, membrane permeability, bioavailability, and activity.[15] The sequential Soxhlet extraction of 30 g of *G. sylvestre* leaf powder in petroleum ether (polarity index = 0.1), chloroform (polarity index = 4.1), and ethyl acetate (polarity index = 4.4) removed most of the hydrophobic phytochemicals such as fatty acids, alkaloids, hydrophobic terpenes, and oils. Subsequent extraction of the residue with methanol (polarity index = 5.1)-extracted amphiphilic compounds such as hydrophilic flavonoids, quinones, terpenoids, tannins, saponin, and coumarins (Table 1). 30 g of leaf powder yielded ∼4 g of the crude methanol extract (CME) that constituted ∼13% (w/w) of the total dry weight of the leaf. Separation of the CME on the Silica-GF254 plate using $CHCl_3$/methanol (1:1 by volume) produced 4−5 indistinct spots, possibly, because of the trailing produced in the presence of acidic compounds (Figure 1A). Acidification of the CME to pH ∼ 1.0 with 2% (w/v) H_2SO_4 yielded 700 mg of the greenish white precipitate that was pelleted down at 7000 rpm and 4 °C. This fraction exhibited solubility in both methanol and HEPES buffer that was termed as the methanol-extracted fraction of *G. sylvestre* (MEFGS). Upon separation on the Silica-GF254 TLC plate using $CHCl_3$/methanol (1:1 by volume) MEFGS that constituted 2.3% (w/w) of the total dry weight of *G. sylvestre* leaves produced a single spot on the TLC plate.

Table 1. Phytochemical Screening of the Crude Extract and MEFGS

tests	CH_3OH (crude)	MEFGS (purified)
terpenoid (Salkowski test)	++	+
glycoside (Keller Killiani test, Molisch's test, and conc. H_2SO_4 test)	−	−
quinone (conc. H_2SO_4 and conc. HCl)	++	−
carbohydrates (Fehling's test and Molisch's test)	−	−
tannin ($FeCl_3$ test and alkaline regent test)	+	−
protein (Biuret test and ninhydrin test)	−	−
saponin (Shinoda test)	−	+
flavonoid (Jone's test)	+	+
coumarin (NaOH test)	+	−
steroid	−	−
alkaloid (Mayer's test, Wagner's test, and tannic acid test)	−	−

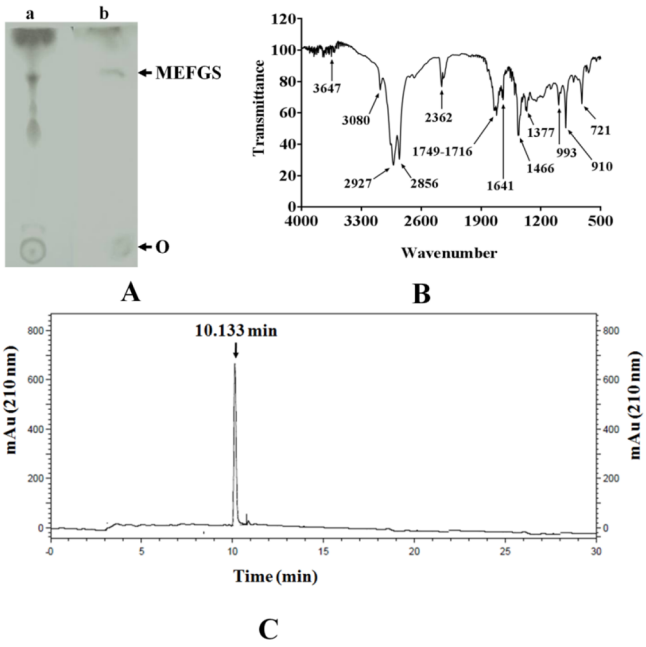

Figure 1. Characterization of the MEFGS (A) TLC showing (a) crude CH_3OH extract (left) and (b) MEFGS fraction (right). "O" denotes the point of sample application. (B) Fourier transform infrared (FTIR) spectrum of the MEFGS. Arrows indicate the peaks identified with their respective wavenumber. (C) High-performance liquid chromatography (HPLC) chromatogram of MEFGS separated using mobile phase H_2O/acetonitrile (80:20) in the C-18 column.

Purification of a single plant compound is laborious and time-consuming. Even the commercial gymnemic acid is a mixture of 18 different analogs, exhibiting a high degree of homology among themselves making their separation a cumbersome procedure.[16] Hence, use of phytochemical mixtures that exhibit a defined bioactivity is more common because of their similar solubility, permeability, and bioavailability.[15] Many phytochemicals with higher hydrophobic indices exhibit elevated *in vitro* antimicrobial activity. However, their *in vivo* therapeutic application becomes limited due to poor solubility in blood. In contrast, aqueous phytochemicals that exhibit higher solubility in blood show poor membrane permeability, resulting in their reduced bioavailability in pathogens. Hence, amphiphilic phytochemicals with high solubility in aqueous solvents and enhanced membrane permeability are more potent herbal therapeutics.[17]

Our study revealed that the sequential extraction of *Gymnema* leaf powder in the order petroleum ether → $CHCl_3$ → ethyl acetate → methanol → precipitation at pH 1.0 is a more effective purification method for amphiphilic

https://doi.org/10.1021/acsomega.1c05581
ACS Omega 2021, 6, 35667−35678

phytochemicals from *G. sylvestre* compared to the single-step extraction by methanol, as described in many earlier studies.[18] 1 kg of *Gymnema* leaf powder yielded 23 g of MEFGS which exhibited ≥50 mg/mL solubility in aqueous buffer at neutral pH.

MEFGS tested positive for the Salkowski test, foam test and Shinoda test, indicating the presence of terpenoids, saponins, and flavonoids, respectively (Table 1). The FTIR transmittance spectrum of MEFGS was similar to that of a terpenoid fraction from *G. sylvestre* (Retz.) R.Br. ex Sm purified in an earlier study.[13] The prominent peaks at 1749−1716 cm^{-1} indicate the characteristic ester linkage in terpenoids[8] (Figure 1B). The broad and prominent peak between 3600 and 3400 cm^{-1} that results from heavily hydrogen bonded −OH groups with surrounding water molecules is absent from MEFGS. However, a low intensity broad peak observed at 3700−3600 cm^{-1} indicates the presence of low-glycosylated terpenoids (e.g., mono-desmosidic triterpene saponins).[19] The FTIR peak at 1641 cm^{-1}, which presents −C═O vibration, is observed for many flavonoids.[20] Upon separation in the C-18 column using H_2O/acetonitrile 80:20 (v/v), MEFGS produced a single chromatogram peak with retention time 10.13 min, indicating homogeneity of the fraction (Figure 1C).

2.2. Identification of Phytochemicals in MEFGS. Total nine different bioactive compounds were identified in MEFGS through a correlation of the molecular ions and the fragmentation patterns produced in liquid chromatography−mass spectrometry (LC−MS) analysis. The LC−MS data were compared with the existing *G. sylvestre* phytochemicals for identification (Table 2). Six terpenoids, two flavonoids, and 1 alkaloid were identified in MEFGS (Figure 2A,B).

Four gymnemic acids identified were gymnemic acid I, IV, VII, and VIII that exhibit high structural homology among themselves (Figure 2A). The major compounds identified in MEFGS were gymnemic acid I, (R_t = 25.17 min) at m/z = 791 and its other three isoforms: gymnemic acid IV (R_t = 25.606 min) at m/z =7 91, gymnemic acid VII (R_t = 1.877 min) at m/z = 713, and gymnemic acid VIII (R_t = 28.665 min) at m/z = 1017.5 (Table 2).[21−25] In addition, two more terpenoids found were the parent compound gymnemagenin (m/z = 492.7) and gymnemic acid derivative 21-*O*-tigloyl (3*β*,16*β*,21*β*,22*α*),3,16,22,23,28 pentahydroxyolean-12-ene-21-yl (2*E*)-2-methylbut-2methylbut-23-enoate (m/z = 565). All gymnemic acids were monodesmosidic triterpene saponins with the oleane skeleton and single glycosyl group (glucoronic acid) at the R_3 position. However, their biological activities differ significantly depending upon the position of functional groups and number of acyl chains.[23] No higher order glycosylated (di and tri-desmosidic) forms of gymnemic acid were observed. The commercial gymnemic acid is a mixture of 18 different analogs which are difficult to purify. They exhibit high degree of similarity among themselves, making their separation a cumbersome procedure.[16] Monodesmosidic saponins exhibit enhanced membranolytic potential compared to di- and tri-desmosidic due to their stronger membrane association.[26]

Two flavonoids, hypolaetin (R_t = 40.328 min) at m/z = 301.5 and aromadendrin (R_t = 41.328 min) at m/z = 287.1, were identified in MEFGS. 8-Hydroxy gymnamine (m/z = 297.2) is the only alkaloid observed in the MEFGS fraction. Percentage of phytoconstituents in MEFGS ranged from 3 to 29%. Out of nine compounds identified from MEFGS, gymnemic acid VIII was predominant at 29.5%. Gymnemic

Table 2. MS Analysis of MEFGS

S.N.	RT	height	area	mass (m/z)	assignment	literature	compounds	References
1	1.877	58,1643	8,901,380	713	$[M + H + 2Na]^-$	$C_{38}H_{58}O_{11}$ 712.6 $[M + 2Na]^+$	gymenmic acid VII	21
2	19.689	821,835	19,343,030	565	$[M-H_2O]^-$	$C_{35}H_{57}O_7$ 589.4 $[M + H]^+$	21-*O*-tigloyl (3*β*,16*β*,21*β*,22*α*),3,16,22, 23,28 pentahydroxyolean-12-ene-21-yl (2*E*)-2-methylbut-gmethylbut-23-enoate	16
3	25.177	877,905	13,069,838	791	$[M-H_2O]^-$	$C_{43}H_{66}O_{14}$ 807.3 $[M-H]^-$	gymnemic acid I or IV	22
4	25.606	2,766,870	48,941,444	791	$[M-H_2O]^-$	$C_{43}H_{66}O_{14}$ 807 .3 $[M-H]^-$	gymnemic acid I or IV	22
5	28.665	540,132	86,433,386	1017.5	$[M-2Na]^-$	$C_{46}H_{76}O_{19}$ 967.8 $[M-H]^-$	gymnemic acids VIII	23
6	40.328	783,491	16,191,299	293.1	$[M-OH]^-$	$C_{15}H_{10}O_7$ 301.5 $[M-H]^-$	hypolaetin	24
7	41.328	387,285	11,802,372	265.1	$[M-H_2O]^-$	287.1 $[M-H]^-$	aromadendrin	24
8	42.925	800,852	12,515,377	297.2	$[M-CO_2]^-$	331.8 $[M-H]^-$	8-hydroxy gymnamine	24
9	45.580	2,300,888	38,268,834	492.7	$[M-H_2O]^-$	505.7 $[M-H]^-$	gymnemagenin	25

https://doi.org/10.1021/acsomega.1c05581
ACS Omega 2021, 6, 35667−35678

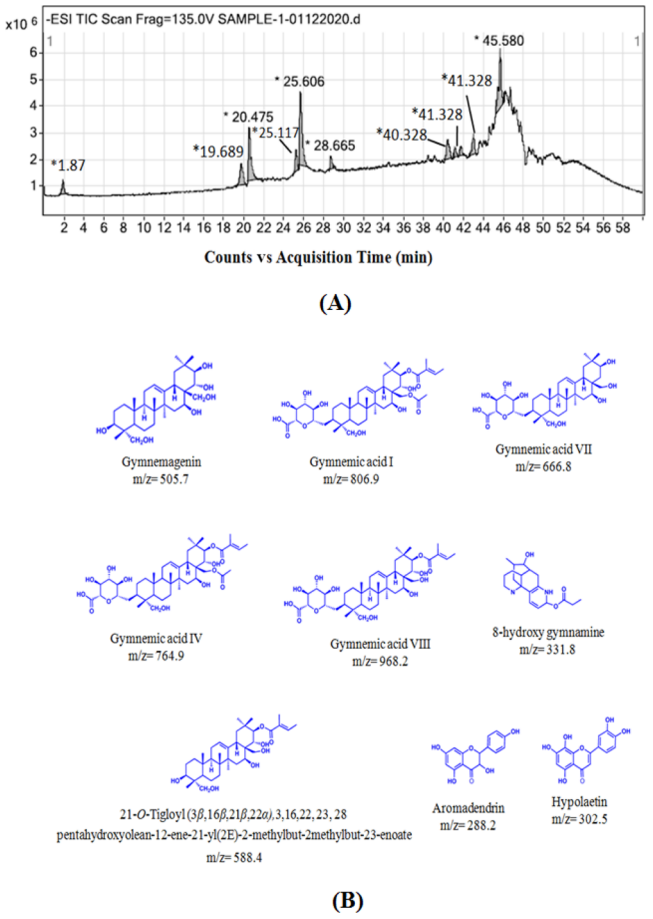

Figure 2. Identification of phytochemicals in MEFGS by mass spectrometry. (A) LC−electrospray ionization (ESI)−MS chromatogram of the MEFGS showing peaks detected in the positive ionization mode (B) Phytochemicals identified in MEFGS based on their charge (z) to mass (m) ratio (m/z). Structures of the compounds were drawn using ChemDraw.

acid I, gymnemagenin and 21-*O*-tigloyl (3β,16β,21β,22α),3,16,22,23,28 pentahydroxyolean-12-ene-21-yl(2*E*)-2-methylbut-2methylbut-23-enoate, acylated oleane lupane triterpenes were found at 16.71, 13.07, and 12.74%, respectively. The flavonoids, hypolaetin and aromadendrin, were found at the concentration of 5.53 and 4.03%, respectively. The 8-hydroxy gymnamine is a minor component that constitutes 4.2 % of MEFGS. All nine phytochemicals identified in MEFGS were amphiphilic with higher solubility in aqueous buffer that increases their suitability for *in vivo* therapeutic applications.

2.3. Lipid-Flipping Activity of MEFGS in LUVs. As amphiphilic compounds exhibit an increased interaction with biological membranes, LUVs were used as a model system for the investigation of their membrane interaction.[5] Electroformation of LUVs on the copper electrode produced unilamellar, mono-dispersed vesicles of 0.25−2.0 μ diameter, which are large enough to be visualized at 1500 X magnification and had a vesicle count of ~3600/mL.[27] (Figure 3A,B). Unilamellarity of the vesicles was determined by the calculation of the unilamellarity index (I_U) that is defined by the following formula

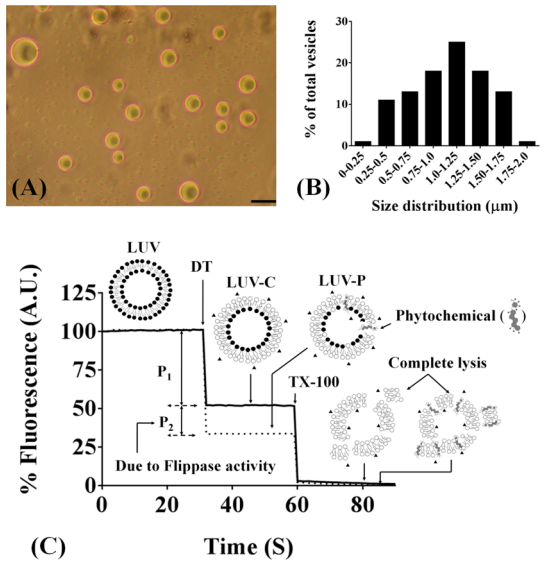

Figure 3. Preparation and characterization of LUVs. (A) Phase contrast image of LUVs at 400× magnification. Scale: 5 μm. (B) Size distribution of LUVs determined by manual counting of 300 vesicles. (C) Schematic diagram showing flippase assay. Normalized initial fluorescence (F_0) of both control (LUV-C) (—) and MEFGS-treated LUVs (LUV-P) (...) is ~100% due to fluorescent NBD-PE (indicated in the dark). Quenching of NBD-PE (indicated in white) by the membrane impermeable dithionite on the outer leaflet decreases F_0 by (P_1 + P_2), where P_1 indicates the fluorescence drop caused due to NBD-fluorescence quenching in the outer leaflet, and P_2 indicates additional fluorescence drop caused due to the flipping of the inner leaflet NBD-PE to the outer membrane leaflet. However, addition of triton-X-100 at 1 min lyses all LUVs, leading to almost complete reduction of NBD fluorescence in LUVs. The residual fluorescence after triton X-100 treatment represents unquenchable fluorescence (F_U).

$$I_U = \frac{\text{fluorescence intensity of NBD-PE in the inner membrane leaflet } (F_i)}{\text{total quenchable fluorescence } (F_T)} \times 100$$

where $F_T = F_0 - F_R$, F_0 = initial fluorescence, F_R = the residual unquenchable fluorescence left after the vesicles were treated with triton X-100. $F_{in} = (F_0 - F_R) - F_o$, where F_o and F_{in} are the NBD fluorescence contributed by the outer and inner membrane of LUVs, respectively.

An I_U value of ~(50 ± 5) % shows that the NBD-PE is equally distributed on both inner and outer leaflets of LUVs, indicating their unilamellar nature (Figure 3C). Induction of lipid flip-flop by *Gymnema* terpenoids is one of the proposed mechanism of their membrano-lytic activity.[13] Lipid flip-flop across the lipid bilayer is a slow process due to the unfavorable energy barrier that a lipid has to overcome when its polar head group moves through the hydrophobic membrane core.[28] Amphiphilic phytochemicals in MEFGS exhibited lipid flippase activity across LUV membranes that was measured by % flipping of NBD-PE from the inner leaflet to the outer leaflet and subsequently quenched by the dithionite. % NBD-PE flipped across the LUV membrane increased linearly with increased doses of MEFGS (Figure 4A). The presence of 100 to 600 μg/mL MEFGS in LUVs that had ~100 μg egg-PC/mL increased the phospholipid/MEFGS (w/w) ratio from 1:1 to 1:6 that resulted in 25% increase in NBD-PE flipping (Figure 4A). This finding suggests that MEFGS phytochemicals interact with LUVs, resulting in the perturbation of the lipid

https://doi.org/10.1021/acsomega.1c05581
ACS Omega 2021, 6, 35667−35678

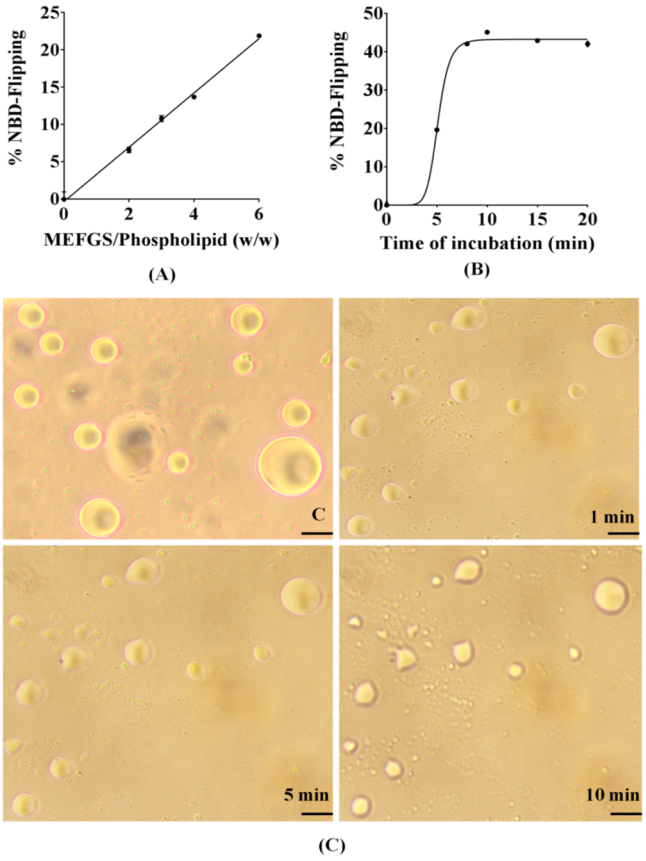

Figure 4. Flippase activity of MEFGS in LUVs. (A) Dose-dependence of % NBD-PE flipping in LUVs by MEFGS. LUVs were incubated with increasing doses of MEFGS at 25 °C for 15 min. (B) % NBD-PE flipping when LUVs were treated with 75 μg MEFGS and incubated for increasing time. (C) Interaction of MEFGS with LUVs led to their distorted morphology, resulting in lysis. Images in the clockwise direction are untreated control (C) (upper left), LUVs treated with 75 μg MEFGS and incubated for 1 min (upper right), 5 min (lower left), and 10 min (lower right).

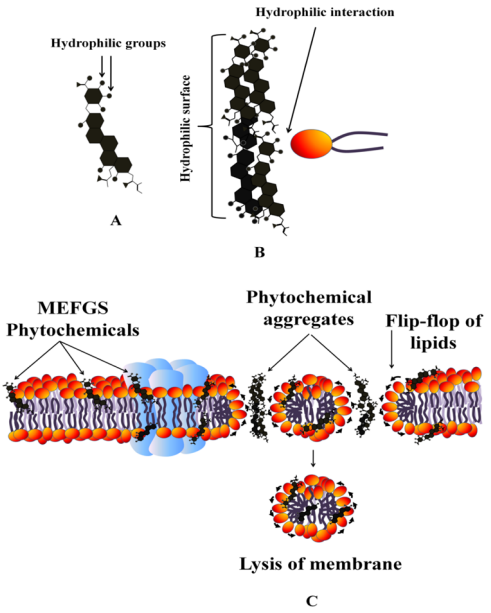

Figure 5. Proposed mechanism of membrane association, lipid flipping, and membrane lysis induced by MEFGS phytochemicals. (A) Phytochemicals in MEFGS possess multiple polar groups attached to a rigid planar ring. (B) Upon membrane association, the phytochemicals possibly form aggregates with their rings stacked together and polar groups projected outward. The polar functional groups interact with the polar head group of membrane lipids. (C) Phytochemical aggregates plausibly induce bilayer defects and form polar surfaces to facilitate flipping of the polar lipid head group across the membrane. Lipid flipping might lead to membrane destabilization and lysis.

bilayer that induces flip-flop of NBD-PE across the membrane. % NBD-PE flipping at an MEFGS/phospholipid (w/w) ratio 2.5 exhibited a sigmoidal relationship with incubation time (Figure 4B).

NBD-PE flipping increased linearly with the MEFGS concentration and exhibited a sigmoid relationship with time that had a saturation rate constant k = (12.09 ± 0.94) mg^{-1} min^{-1}. At egg-PC/MEFGS (w/w) ratio 2.5, the flippase activity was saturated at ~10 min with ~40% NBD-PE flipping from the inner leaflet to the outer leaflet. An initial slow rate of the interaction between MEFGS components with LUVs increased exponentially with time, resulting in the saturation of NBD-PE flipping. These results indicate that phytochemicals in MEFGS cooperatively associate with the LUV lipid bilayer in a concentration- and time-dependent manner that probably results in the formation of lipid-flipping complexes (Figure 5). A variety of molecular species that induce defects in the lipid bilayer could induce lipid flip-flop in the biological membrane.[29,30] Accordingly, proteins (e.g., GPCRs and scramblases), peptides (e.g., gramicidin), and non-bilayer forming lipids (e.g., ceramides and oxidized lipids) are potential flippases.[29,31,32] However, their kinetics and mechanism of action differ significantly depending upon the nature of the flippase molecule and its membrane association. Saponins partially permeate into biomimmetic membranes beyond their critical micelle concentrations with the hydrophilic moiety protruding out of the membrane and hydrophobic tail penetrating the bilayer.[33]

Protein flippases such as opsins form hydrophilic surfaces to facilitate the movement of hydrophilic lipid head groups.[34] However, individual phytochemicals are of insufficient dimension to span the entire membrane bilayer that is required to form a trans-membrane pathway for membrane lipid flipping (Figure 5). In contrast, the phytochemical aggregates in the membrane bilayer plausibly provide the hydrophilic surfaces that facilitate the transbilayer movement of the hydrophilic lipid head group across the bilayer.[13,30−32] Binding of MEFGS components to LUVs altered their rounded morphology, as detected by phase contrast microscopy (Figure 4C). The untreated control LUVs are rounded in shape with smooth surfaces, whereas treatment with MEFGS at an MEFGS/phospholipid (w/w) ratio of 2.5 led to the time-dependent change in vesicle shape, resulting in their irregular morphology. This result confirms a time-dependent interaction of MEFGS phytochemicals with the LUVs, leading to their destabilization, probably resulting in their lysis.

2.4. MEFGS Enhances the Permeability of the Bacterial Membrane. MEFGS treatment of bacteria increased their permeability to crystal violet, leakage of cytosolic phosphates, ions (P < 0.001), and proteins (P < 0.001) (Figure 6). Incubation of *Escherichia coli*, *Staphylococcus aureus*, and *Pseudomonas aeruginosa* at increasing doses (0.1, 0.2, and 0.4 mg/mL) of MEFGS enhanced the entry of crystal violet by 23, 17, and 17%, respectively, compared to their

https://doi.org/10.1021/acsomega.1c05581
ACS Omega 2021, 6, 35667−35678

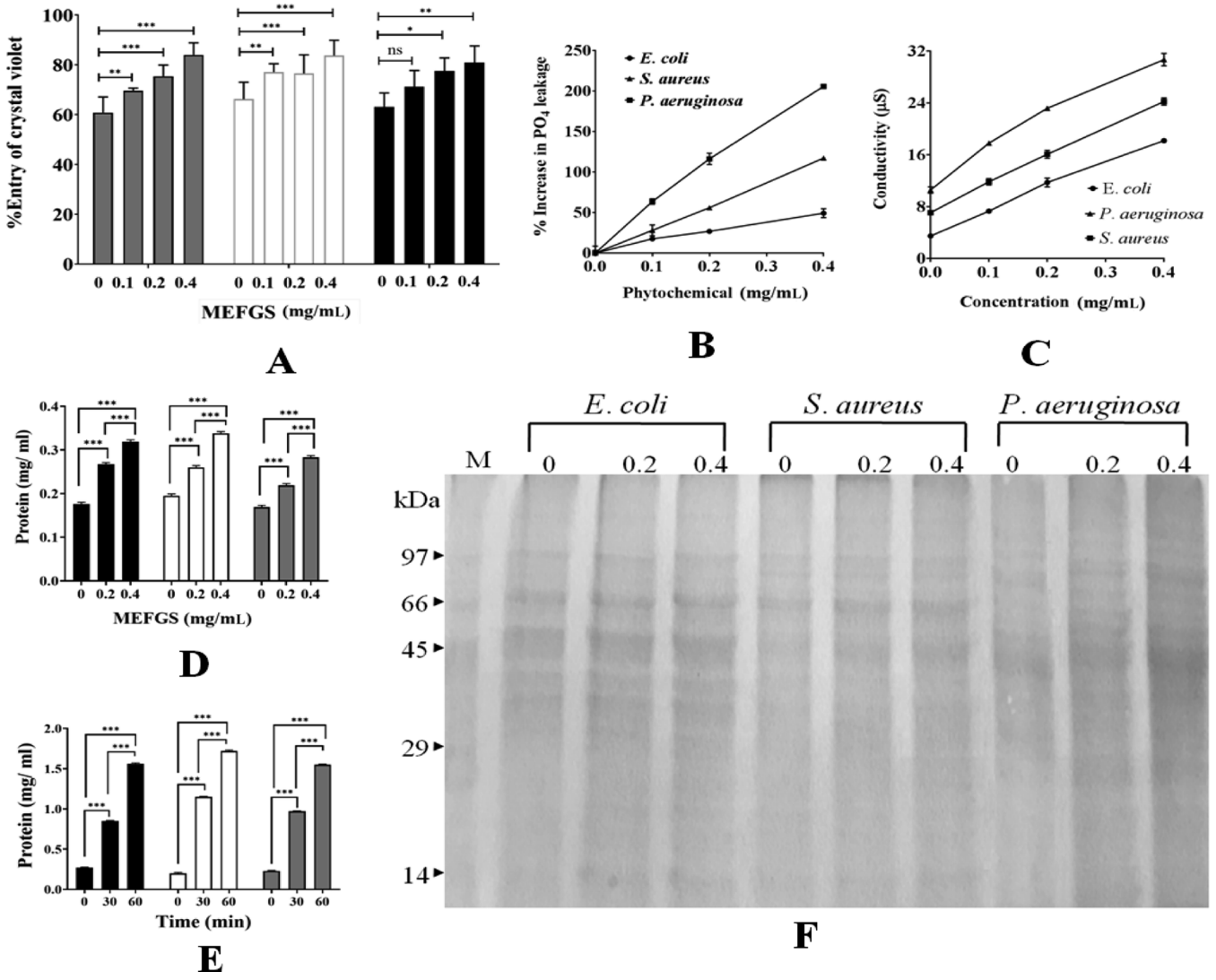

Figure 6. Increase in membrane permeability of bacteria when treated with increasing doses (mg/mL) of MEFGS for 30 min at 37 °C. (A) % Uptake of crystal violet when *E. coli* (gray bars), *S. aureus* (white bars), and *P. aeruginosa* (black bars) were treated with increasing doses (0, 0.1, 0.2, and 0.4 mg/mL) of MEFGS. (B) % increase in PO_4^{3-} leakage when *E. coli*, *P. aeruginosa*, and *S. aureus* were treated with increasing doses (0, 0.1, 0.2, and 0.4 mg/mL) of MEFGS. (C) Increase in electrical conductivity of the extracellular medium due to the leakage of cellular ions when *E. coli*, *P. aeruginosa*, and *S. aureus* were treated with increasing doses (0, 0.1, 0.2, and 0.4 mg/mL) of MEFGS. Dose-dependent (D) and time-dependent (E) increase in leakage of cellular proteins into the extracellular medium when *E. coli* (black), *P. aeruginosa* (white), and *S. aureus* (gray) were treated with increasing doses of MEFGS. (F) Sodium dodecyl sulphate-polyacrylamide gel electrophoresis (SDS-PAGE) showing a dose-dependent increase in the extracellular protein content when the bacteria were treated with increasing doses (0, 0.2, and 0.4 mg/mL) of MEFGS, as indicated on top of the gel. "M" denotes a molecular-weight marker (Bio-Rad).

untreated controls (Figure 6A) ($P < 0.0001$). An increase in crystal violet permeability into bacteria is an indicator of phytochemical-induced membrane damage.[35] Corilagin, a polyphenolic tannin, enhances the permeability of crystal violet into *E. coli* and *Candida albicans*.[36] Essential oil from *Fructus forsythia* shows antimicrobial activity against *E. coli* and *S. aureus* by increasing their membrane permeability, as indicated by 35 and 60% enhanced uptake of crystal violet.[37] Our study shows that the flip-flop-inducing amphiphilic molecules from *G. sylvestre* are milder membrane permeabilizing agents compared to essential oils that increases their therapeutic potential. Leakage of cellular PO_4^{3-} and proteins due to the increased membrane permeability is one of the primary mechanisms of phytochemical induced anti-bacterial activity.[38]

Incubation of *E. coli*, *S. aureus*, and *P. aeruginosa* at increasing doses (0.1, 0.2, and 0.4 mg/mL) of MEFGS proportionately enhanced the PO_4^{3-} content of the extracellular medium up to 50, 117, and 205%, respectively, compared to the untreated controls ($P < 0.001$) (Figure 6B). This leaked PO_4^{3-} content represents the sum of organic (e.g., ATP) and inorganic PO_4^{3-}, indicating enhanced permeability of bacterial membranes to phosphates. Leakage of organic phosphates such as ATP, ADP, AMP and nucleotides into the extracellular medium is a major contributor of extracellular phosphates. For example, essential oil from black pepper enhanced ATP release from *E. coli* by 6–13 times.[39] Relative leakage of PO_4^{3-} was in order *P. aeruginosa* > *S. aureus* > *E. coli*, indicating differences in their cytosolic PO_4^{3-} concentration or differential action of MEFGS phytochemicals on their membranes due to different membrane lipid compositions.[40] Treatment of bacteria with

https://doi.org/10.1021/acsomega.1c05581
ACS Omega 2021, 6, 35667−35678

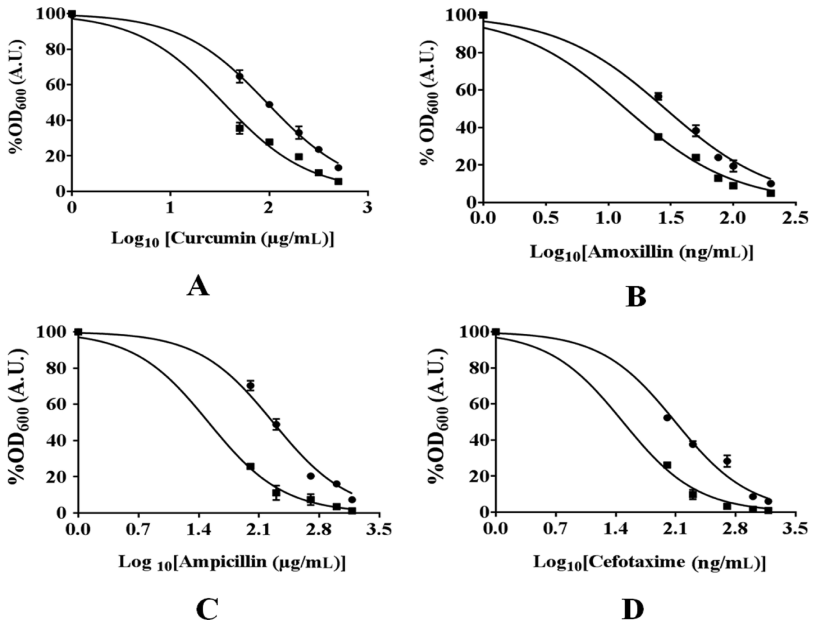

Figure 7. Effect of MEFGS on the efficacy of antimicrobials on *S. aureus*. Dose−response curves showing growth (OD_{600}) of *S. aureus* at 37 °C for 18 h when incubated directly with increasing doses of antimicrobials (circle) or after pretreatment with 0.2 mg/mL MEFGS (square): (A) curcumin, (B) amoxicillin, (C) ampicillin, and (D) cefotaxime. At least three independent sets of data were analyzed using graph pad prism (version 6).

Table 3. Effect of MEFGS on the Efficacy of Anti-*S. aureus* Compounds[a]

	IC_{50}						
antimicrobial	no. MEFGS	+0.2 mg/mL MEFGS	MEFGS (μg/mL)	FIC_{50} of antimicrobial	FIC_{50} of MEFGS	$FIC_{50}I$	effect
curcumin	94.08 μg/mL	34.00 μg/mL	354.87	0.361	0.096	0.457	S
ampicillin	183.70 ng/mL	32.67 ng/mL	354.87	0.178	0.092	0.270	S
amoxillin	28.58 ng/mL	13.79 ng/mL	354.87	0.483	0.039	0.521	P
cefotaxime	124.70 ng/mL	30.51 ng/mL	354.87	0.245	0.086	0.331	S

[a]Effects of MEFGS on efficacy of antimicrobials *in vitro* were quantified by determining the fractional inhibitory concentration (FIC) for individual antimicrobials. The FIC_{50} index ($FIC_{50}I$) was calculated using the following formula: $FIC_{50}I = FIC_{50}IA + FIC_{50}IB = [(IC_{50(A)}/IC_{50\ (A+B)}) + (IC_{50(A)}/IC_{50\ (A+B)})]$. The effect was considered synergistic (S) when $FIC_{50}I < 0.5$ and partially synergistic (P) when $FIC_{50}I$ is from 0.5−0.75.

increasing doses (0.1, 0.2, and 0.4 mg/mL) of MEFGS led to a linear increase in ionic conductivity of the extracellular medium of *E. coli*, *S. aureus*, and *P. aeruginosa* up to 5.0-, 3.5-, and 3.0-fold, respectively, compared to the untreated controls ($P < 0.001$) (Figure 6C). Phytochemical-mediated membrane perturbation is the most accepted mechanism of their cytosolic ion leakage inducing effects on bacteria. In addition, inhibition of mechanosensitive ion channels, voltage-gated K^+-ion channels, and dissipation of membrane potential together contribute to the leakage of cytosolic ions.[41] This finding indicates that the MEFGS phytochemicals increase ionic permeability of bacterial membranes. The membrane permeabilizing action of MEFGS on bacteria was further confirmed by analysis of cytosolic protein leakage into the extracellular medium. Incubation of *E. coli*, *S. aureus,* and *P. aeruginosa* with MEFGS led to dose-dependent ($P < 0.001$) and time-dependent ($P < 0.001$) enhancement in leakage of cytosolic proteins into the extracellular medium (Figure 6D,E). MEFGS-induced increased leakage of cellular proteins was detected on 10% SDS-PAGE (Figure 6D). These findings suggest that the flippase-inducing phytochemicals in MEFGS disrupt bacterial membranes, leading to the leakage of cytosolic proteins into the extracellular medium.

2.5. MEFGS Phytochemicals Enhance the Efficacy of Antimicrobials on *S. aureus*. MEFGS was bacteriostatic with a growth inhibitory effect on three common human pathogens, *S. aureus* (MTCC-212) (IC_{50} = 0.355 mg/mL), *P. aeruginosa* (MTCC-1035) (IC_{50} = 0.1 mg/mL), and *E. coli* (MTCC-118) (IC_{50} = 0.5 mg/mL), showing that the MEFGS phytochemicals exhibit moderate anti-bacterial activity. However, MEFGS significantly enhanced the efficacy of common antimicrobials on *u* probably by increasing their membrane permeability. (Figure 7). Incubation of *S. aureus* with curcumin, amoxillin, ampicillin, or cefotaxime in the presence of 0.2 mg/mL MEFGS reduced their IC_{50} values by 3, 2, 6, and 4 fold, respectively (Table 3).

Calculation of FIC exhibited by each antimicrobial showed synergistic action of MEFGS on curcumin, ampicillin, and cefotaxime. However, MEFGS exhibited partial synergy with amoxillin. Bacterial membranes act as barriers that inhibit entry of antimicrobials to reach their cellular targets. Membrane permeability enhancers increase the efficacy of antimicrobials by facilitating their bioavailability inside the microbe.[42] (Figure 7). The enhanced antimicrobial efficacy could be explained by their MEFGS-induced increase in permeability into *S. aureus*. Similar activity enhancement was observed for aminoglyco-

https://doi.org/10.1021/acsomega.1c05581
ACS Omega 2021, 6, 35667−35678

sides and β-lactam antibiotic activity when co-treated with essential oil from *Lippia sidoides* and thymol.[43]

Natural outer membrane permeabilizers boost antibiotic action against irradiation-resistant bacteria.[44] Membranotropic phytochemicals also enhance the antimicrobial efficacy through inhibition of membrane-localized efflux pumps (e.g., MDR) that reduces cytosolic accumulation of drugs to the lethal concentration.[3] However, activities of MDR and other membrane-associated resistance factors are dependent upon the lipid microenvironment that is disrupted by the phytochemical−membrane interaction that might account for the observed antimicrobial efficacy. However, further studies are required to determine any specific interaction of MEFGS components with membrane proteins.

2.6. Hemolytic Effect of MEFGS. As the phytochemicals in MEFGS exhibit membranotropic activity on bacteria, we investigated its hemolytic effect on human erythrocytes. MEFGS from 0.1 to 0.4 mg/mL exhibited less than 2% hemolytic activity on human erythrocytes (Figure 8).

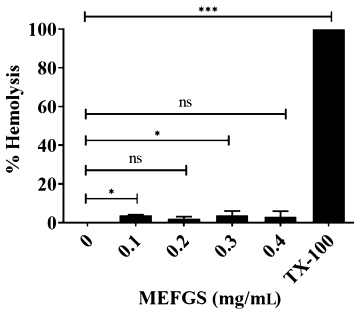

Figure 8. Hemolytic activity of MEFGS. % hemolysis of human erythrocytes induced by increasing doses of MEFGS. The lysis induced by 1% Triton X-100 (TX-100) was 100%. TX-100 was used as a positive control, and PBS was taken as a negative control.

Increasing doses (0.1−0.4 mg/mL) of MEFGS exhibited no significant ($P > 0.05$) hemolytic effect on human erythrocytes. These results indicate that MEFGS components exhibit membranolytic activity on the bacterial membrane, however, without any significant lytic effect on human erythrocytes. The absence of hemolytic activity of MEFGS components increases their potential as therapeutic agents for human consumption.

Our study reveals that MEFGS, that is a mixture of membranotropic terpenoids, flavonoids, and alkaloids, perturbs bacterial membrane integrity by inducing flip-flop of membrane lipids. However, the observed activity could have originated from a single compound or from the combined action of multiple phytochemicals in MEFGS. Flippase activity is exhibited by the diverse variety of molecules such as organelle extracts, proteins, lipids, and phytochemicals.[13,34,45] In contrast to protein flippases, flip-flop-inducing phytochemicals lead to membrane destabilization that could be explored further for the therapeutic application of these molecules. However, purification of individual phytochemical constituents in MEFGS and analysis of their flippase activity will reveal their specific mechanism of membrane-destabilizing behavior.

3. CONCLUSIONS

In conclusion, our study identified amphiphilic phytochemicals from the methanol-extracted fraction of *G. sylvestre* that exhibited flip-flop of NBD-PE in LUVs. The flippase-inducing phytochemicals exhibited concentration- and time-dependent interactions with the lipid bilayer, resulting in membrane perturbation. Lipid-flipping activity of MEFGS was accompanied by enhanced permeability of the bacterial membrane to crystal violet, ions, phosphates, and proteins. MEFGS synergistically enhanced the efficacy of antimicrobials against *S. aureus* plausibly by increasing their permeability into the bacterium. The phytochemicals exhibited high solubility in aqueous medium and negligible hemolytic activity that potentiates their therapeutic application. For the first time, our study reveals that the flip-flop-inducing phytochemicals from *G. sylvestre* enhance the permeability of bacterial plasma membranes by facilitating trans-bilayer movement of lipids.

4. MATERIALS AND METHODS

4.1. Chemicals and Microbial Cultures. *N*-(7-Nitrobenz-2-oxa-1,3-diazol-4-yl)-1,2-dihexadecanoyl-*sn*-glycero-3-phosphoethanolamine, triethylammonium salt (NBD-PE) (lyophilized powder) and egg-phosphatidylcholine (egg-PC) (100 mg/mL in $CHCl_3$) were purchased from Sigma (India). LB medium and antibiotics were purchased from Himedia, India. DMSO, KBr, silica GF-254, dithionite, ammonium molybdate, ascorbic acid, crystal violet, all organic solvents, ninhydrin reagents, and routine chemicals were purchased from Merck (India).

4.2. Bacteria and Culture Condition. *S. aureus* (MTCC-212), *E. coli* (MTCC-118), and *P. aeruginosa* (MTCC-1035) were obtained from the Microbial Type Culture Collection (MTCC), Institute of Microbial Technology (IMTECH), Chandigarh, India. Bacteria were maintained in LB agar medium and grown in liquid LB at 200 rpm and 25 °C

4.3. Isolation of MEFGS. Healthy leaves of *G. sylvestre* (Retz.) R.Br. ex Sm were collected from Similipal Biosphere Reserve and identified at Regional Plant Research Center, Bhubaneswar, Odisha. The plant was deposited in the herbarium center with specimen voucher number 8386. Phytochemical extraction was performed following the method described earlier.[46] Briefly, 30 g of leaf powder was sequentially extracted at 45 °C in order petroleum ether → $CHCl_3$ → CH_3OH, for 35 cycles in each solvent using Soxhlet apparatus. The CME (∼300 mL) was dried in a rotary evaporator (Bucchi, Japan, model R-300), and 300 mg was dissolved in 100 mL of methanol; pH was adjusted to 1.0 using concentrated H_2SO_4. The greenish white precipitate was collected by centrifugation at 12,000 rpm and 4 °C for 15 min and washed twice with absolute ethanol. The precipitate was air dried at 25 °C, dissolved at 10 mg/mL in resuspension buffer (10 mM HEPES, 100 mM NaCl, pH 7.6), and stored at 4 °C for further analysis. This fraction was termed as MEFGS. Purity of the fraction was analyzed on silica gel GF254 TLC plates and HPLC.

4.4. Phytochemical and Spectroscopic Characterization. Phytochemical analysis of MEFGS was performed, as described by Ejikeme.[47] Chemical bonds associated with the functional groups were determined by scanning the transmittance of MEFGS using a FTIR spectrophotometer (Shimadzu, IR Affinity 1, Japan).[48] Briefly, 2 mg of the purified fraction mixed with KBr at 2:98 (w/w) was prepared as solid pellets and scanned from 4000 to 400 cm^{-1} at 4 mm/s and 2 cm resolution. Homogeneity of the MEFGS was determined by HPLC (Shimadzu, Japan) using the C-18 column in H_2O/acetonitrile (80:20) (v/v).

4.5. LC−MS Analysis. Phytochemical constituents of MEFGS was determined using a Shimadzu LC−MS 2020

https://doi.org/10.1021/acsomega.1c05581
ACS Omega 2021, 6, 35667−35678

system equipped with a binary pump (LC-20ADXR).[49] The chromatographic separation was performed using an AQUASIL C18 analytical column (150 mm × 3 mm × 3 μm particle size) using methanol/formic acid at a ratio 99.7:0.3 as the mobile phase with a flow rate of 0.1 mL/min. The photodiode array detector was set at 350 nm for acquiring chromatograms. The injection volume was 20 μL, and peaks were monitored at 250 nm. The LC was interfaced with a Q-TOF mass spectrometer fitted with an ESI source for the determination of mass spectra. Mass spectra were recorded in the positive ionization mode for the mass/charge (m/z) ratio range 50−1500. The temperature of drying gas (N_2) was 400 °C at a gas flow rate of 12 mL/min and nebulizing gas (N_2) pressure of 40 psi. The specific negative ionization modes (m/z $[M-H]^-$) were used to analyze the compounds. The mass fragmentations were identified using spectrum database for organic compounds.

4.6. Determination of Antimicrobial Activity. Antimicrobial activity of MEFGS was evaluated by determining its IC_{50} values on *S. aureus* (MTCC-212), *E. coli* (MTCC-118), and *P. aeruginosa* (MTCC-1035).[50] Briefly, 10^5 colony forming units of bacteria from fresh seed were added to each well. MEFGS was added at the final concentrations 10, 5, 1, 0.5, 0.1, and 0.01 mg/mL, and growth of bacteria was monitored for a period of 24 h at 37 °C. Bacterial growth was determined by measuring their OD_{600} using a UV−visible spectrophotometer (JENWAY 6850). The normalized OD_{600} of bacteria was fitted against $\log_{10}$[concentration] of MEFGS using graph-pad Prism (Version 6) to determine their IC_{50} values. The IC_{50} was defined as the concentration of MEFGS required for 50% growth inhibition.

4.7. Preparation and Characterization of LUVs. LUVs were prepared following the electroformation method.[13] Briefly, a mixture of 0.1 mg (∼130 nmol) egg-PC and 1.5 mol % NBD-PE in $CHCl_3$ was deposited on a copper electrode of the electroformation chamber and dried under a stream of nitrogen so as to remove any trace of $CHCl_3$. The chamber was filled with low salt solution (LSS) (10 mM KCl and 100 mM sucrose), and LUVs were formed by passing alternating current of 10 Hz and 1.5 V for 2 h at 25 °C using a transformer. The LUVs were detached from the electrode by changing the frequency of AC current to 5 V for 30 min. LUVs were characterized by phase contrast imaging using a Nikon inverted microscope (Eclipse Ti−U, Japan) at 1000× magnification, and their mean diameter was determined using NIS-Element software package (version 64 bit) provided by Nikon. Unilamellarity of LUVs was determined by calculating the unilamellarity index (I_U) defined as $I_U = (F_i/F_T)\times 100$, where F_i and F_T represent fluorescence signals emanating from the NBD-PE localized to the inner leaflet and total quenchable fluorescence in LUVs, respectively.

4.8. Lipid Flip-Flop Assay. MEFGS-induced lipid flip-flop was quantitated by measuring the flipping of fluorescent phospholipid analog NBD-PE in LUV membranes.[45] A schematic diagram of the lipid flip-flop assay is given in Figure 3C. Briefly, LUVs (∼10 nmol PO_4) were incubated at increasing doses of MEFGS at 25 °C in 300 μL low salt buffer. The stabilized initial fluorescence (F_0) was recorded using an Agillent JASCO FP-6500 spectrofluorimeter (Japan) (refer to Figure 3C). At 1 min, 10 μL of 1 M sodium dithionite in freshly prepared 1 M Tris-base (pH = 10.5) was added, and the fluorescence signal was monitored for 2 min to quench the dithionite-accessible NBD fluorescence ($P_1 + P_2$) in intact LUVs, where P_1 is the fluorescence drop in untreated controls and P_2 is the additional fluorescence drop in MEFGS-treated LUVs. This additional fluorescence drop (P_2) is due to the MEFGS-induced flipping of NBD-PE from the inner leaflet of LUVs to the outer leaflet, which is measured using the formula

$$A = ([(P_1 + P_2)_{MEFGS}] - [(P_1 + P_2)_{Control}])/F_T \times 100$$

where A is the flippase activity induced by MEFGS and F_T = total quenchable fluorescence in the sample. F_T is determined by adding 20 μL 1% (w/v) Triton-X-100 at 3 min to lyse the LUVs that resulted in quenching of the residual NBD fluorescence emanating from the inner leaflet. $F_T = F_0 - F_R$, where F_0 and F_R represent the initial fluorescence and F_R = residual fluorescence of LUVs after triton X-100 treatment.

4.9. Bacterial Membrane Permeability Assay. Membrane permeability in bacteria was quantitated by crystal violet permeability and leakage of cytosolic ions, phosphates, and proteins. Crystal violet uptake assay was performed following an earlier protocol.[51] Briefly, 1.6×10^7 bacterial cells were mixed with increasing doses of MEFGS in 0.2 mL of resuspension buffer (10 mM Tris−HCl, pH 7.6) and incubated at 37 °C for 30 min. Cells were collected at 10,000 rpm for 5 min at 25 °C, washed in resuspension buffer, and incubated with 10 μg/mL crystal violet in same buffer for 10 min at 37 °C. Percentage crystal violet absorbed by the bacteria was calculated from A_{590} of the supernatant. Release of the total cytosolic ion was quantitated by measuring electrical conductivity of the supernatant.[52] Briefly, 8×10^7 cells were added with increasing doses of MEFGS in 1 mL of resuspension buffer and incubated at 37 °C for 30 min. The supernatant was collected by centrifugation at 10,000 rpm for 5 min at 25 °C, and its ionic conductivity was measured using a Systronics M371 conductivity meter. For phosphate estimation, 100 μL of the supernatant was incubated with 400 μL perchloric acid at 200 °C for 2 h to release the bound PO_4. Total released PO_4 was then added with 2.5% (w/v) ammonium molybdate in the presence of 5% (w/v) ascorbic acid and incubated at 100 °C. The PO_4 content was quantitated from the KH_2PO_4 standard curve by measuring the absorbance of the blue colored ammonium phosphomolybdate complex at 797 nm.[53] Dose-dependent and time-dependent leakage of cytosolic proteins were quantitated using the Lowry method and detected on SDS-PAGE.[54] For dose-dependent assay, 8×10^7 bacteria were treated with increasing doses (0, 0.2, and 0.4 mg/mL) of MEFGS in 0.2 mL of PBS. However, for time-dependent assay, the cells were treated with 0.4 mg/mL MEFGS in 0.2 mL of PBS for increasing (0, 30, and 60 min) time. The bacteria-free supernatant from each sample was precipitated with 100% (w/v) TCA, and the pellet was collected by centrifugation at 12,000 rpm for 30 min at 4 °C. The precipitate was resuspended in 20 μL of PBS. Protein estimation was performed the by Lowry method and qualitatively analyzed on 10% SDS-PAGE.

4.10. Hemolysis Assay. Hemolytic activity of MEFGS was determined by spectrophotometric assay.[55] Briefly, 5 mL of blood was drawn from a healthy individual and centrifuged at 3000 rpm for 3 min. Pellet containing erythrocytes were washed three times with sterile PBS (pH 7.2) and resuspended with 20 packed cell volumes of 0.5% normal saline. 0.19 mL of resuspended erythrocytes was added with 10 μL of MEFGS in PBS at the final concentrations 0, 50, 100, 150, 200 μg/mL and incubated at 37 °C for 30 min. The supernatant was collected at 3000 rpm for 10 min at 25 °C, and relative

https://doi.org/10.1021/acsomega.1c05581
ACS Omega 2021, 6, 35667−35678

hemolytic activity induced by MEFGS was calculated by measuring its absorbance at 540 nm using a UV−visible spectrophotometer (JENWAY 6850). PBS and triton X-100 were used as negative and positive controls, respectively. The study protocol was in compliance with the Helsinki Declaration.

4.11. Effect of MEFGS on the Efficacy of Antimicrobials on *S. aureus*. The effect of MEFGS on anti-*S. aureus* activities of curcumin, amoxillin, ampicillin, and cefotaxime was determined by measuring their half maximal inhibitory concentration (IC_{50}) in 96-well plates.[56] Briefly, 10^5 CFU of *S. aureus* was inoculated in 0.2 mL of LB containing increasing doses of the above antimicrobials in the presence or absence of 0.2 mg/mL MEFGS. The cells were incubated for 18 h at 37 °C. To determine the anti-*S. aureus* effect of MEFGS alone, cells were grown in the presence of 0.2 mg/mL MEFGS under same culture condition in the absence of antimicrobials. Bacteria were collected by centrifugation at 10,000 rpm for 5 min at 25 °C, washed in distilled water to remove traces of LB, and resuspended in 3 mL of distilled water. Bacterial growth was determined by measuring their OD_{600} using a UV−visible spectrophotometer (JENWAY 6850). The normalized OD_{600} of *S. aureus* was fitted against $\log_{10}$[concentration] for each antimicrobial activity using graph-pad Prism (Version 6) to determine their IC_{50} values.

4.12. Statistical Analysis. All experiments were performed at least three times ($N \geq 3$). Data are presented as mean ± SD. All statistical testing were performed using one-way analysis of variance for multiple comparison analyses, whereas Student's *t* test was employed for direct comparison between two data sets using graph pad prism (version 6). Data sets were considered to be statistically significant when $P \leq 0.5$.

AUTHOR INFORMATION

Corresponding Author

Santosh Kumar Sahu − *Department of Biotechnology, Maharaja Sriram Chandra Bhanj Deo University (Erstwhile: North Orissa University), Baripada, Odisha 757003, India;* orcid.org/0000-0002-5141-8103; Phone: +91 9178737281; Email: drsantoshnou@gmail.com

Authors

Himadri Gourav Behuria − *Department of Biotechnology, Maharaja Sriram Chandra Bhanj Deo University (Erstwhile: North Orissa University), Baripada, Odisha 757003, India*

Gandarvakottai Senthilkumar Arumugam − *Bioengineering and Drug Design Lab, Department of Biotechnology, IIT Madras, Chennai 6000 36, India;* orcid.org/0000-0003-4210-0125

Chandan Kumar Pal − *Department of Chemistry, Maharaja Sriram Chandra Bhanj Deo University (Erstwhile: North Orissa University), Baripada, Odisha 757003, India*

Ashis Kumar Jena − *Department of Chemistry, Maharaja Sriram Chandra Bhanj Deo University (Erstwhile: North Orissa University), Baripada, Odisha 757003, India*

Complete contact information is available at: https://pubs.acs.org/10.1021/acsomega.1c05581

Author Contributions

The authors and their respective contribution to the study are as follows. H.G.B. and S.K.S. conceived and designed research. H.G.B. and C.K.P. conducted experiments. G.S.A. and A.K.J. contributed new analytical tools for the identification of compound. H.G.B. and S.K.S. analyzed data and wrote the manuscript. S.K.S has contributed in supervision, conceptualization, and project administration. All authors read and approved the manuscript.

Funding

This study was funded by the Department of Science and Technology, India (grant number—IF160217, INSPIRE Fellowship).

Notes

The authors declare no competing financial interest.

This article does not contain any studies with human participants or animals performed by any of the authors.

Data availability statement: The data sets generated during and/or analyzed during the current study will be available upon reasonable request.

ACKNOWLEDGMENTS

The present work is supported by the Fund for Improvement of S&T Infrastructure in Universities and Higher Educational Institutions (FIST) program under the Department of Science and Technology (DST), India.

REFERENCES

(1) Ayaz, M.; Ullah, F.; Sadiq, A.; Ullah, F.; Ovais, M.; Ahmed, J.; Devkota, H. P. Synergistic interactions of phytochemicals with antimicrobial agents: Potential strategy to counteract drug resistance. *Chem.-Biol. Interact.* **2019**, *308*, 294−303.

(2) Matamoros-Recio, A.; Franco-Gonzalez, J. F.; Forgione, R. E.; Torres-Mozas, A.; Silipo, A.; Martín-Santamaría, S. Understanding the Antibacterial Resistance: Computational Explorations in Bacterial Membranes. *ACS Omega* **2021**, *6*, 6041−6054.

(3) Dias, C.; Rauter, A. P. Membrane-targeting antibiotics: recent developments outside the peptide space. *Future Med. Chem.* **2019**, *11*, 211−228.

(4) Efferth, T.; Koch, E. Complex interactions between phytochemicals. The multi-target therapeutic concept of phytotherapy. *Curr. Drug Targets* **2011**, *12*, 122−132.

(5) Tsuchiya, H. Membrane interactions of phytochemicals as their molecular mechanism applicable to the discovery of drug leads from plants. *Molecules* **2015**, *20*, 18923−18966.

(6) Arun, L. B.; Arunachalam, A. M.; Arunachalam, K. D.; Annamalai, S. K.; Kumar, K. A. In vivo anti-ulcer, anti-stress, anti-allergic, and functional properties of Gymnemic Acid Isolated from Gymnema sylvestre R Br. *BMC Complementary Altern. Med.* **2014**, *14*, 70.

(7) Khan, F.; Sarker, M. M. R.; Ming, L. C.; Mohamed, I. N.; Zhao, C.; Sheikh, B. Y.; Tsong, H. F.; Rashid, M. A. Comprehensive review on phytochemicals, pharmacological and clinical potentials of Gymnema sylvestre. *Front. Pharmacol.* **2019**, *10*, 1223.

(8) Di Fabio, G.; Romanucci, V.; Zarrelli, M.; Giordano, M.; Zarrelli, A. C-4 gem-dimethylated oleanes of Gymnema sylvestre and their pharmacological activities. *Molecules* **2013**, *18*, 14892−14919.

(9) Arora, D. S.; Sood, H. In vitro antimicrobial potential of extracts and phytoconstituents from Gymnema sylvestre R. Br. leaves and their biosafety evaluation. *AMB Express* **2017**, *7*, 115.

(10) Osbourn, A. E. Preformed antimicrobial compounds and plant defense against fungal attack. *Plant Cell* **1996**, *8*, 1821.

(11) Harmatha, J. Chemo-ecological role of spirostanol saponins in the interaction between plants and insects. *Saponins in Food, Feedstuffs and Medicinal Plants*, Oleszek, W., Marston, A., Eds.; Kluwer Academic Publishers: Netherlands, 2000; pp 129−141.

(12) Hemaiswarya, S.; Kruthiventi, A. K.; Doble, M. Synergism between natural products and antibiotics against infectious diseases. *Phytomedicine* **2008**, *15*, 639−652.

(13) Behuria, H. G.; Sahu, S. K. An anti-microbial Terpenoid fraction from Gymnema sylvestre induces flip-flop of fluorescent-

phospholipid analogs in model membrane. *Appl. Biochem. Biotechnol.* **2020**, *192*, 1331−1345.
(14) Bernardes, N.; Fialho, A. Perturbing the dynamics and organization of cell membrane components: a new paradigm for cancer-targeted therapies. *Int. J. Mol. Sci.* **2018**, *19*, 3871.
(15) Barbieri, R.; Coppo, E.; Marchese, A.; Daglia, M.; Sobarzo-Sánchez, E.; Nabavi, S. F.; Nabavi, S. M. Phytochemicals for human disease: An update on plant-derived compounds antibacterial activity. *Microbiol. Res.* **2017**, *196*, 44−68.
(16) Zarrelli, A.; Ladhari, A.; Haouala, R.; Di Fabio, G.; Previtera, L.; DellaGreca, M. New acylated oleanane and lupane triterpenes from Gymnema sylvestre. *Helv. Chim. Acta* **2013**, *96*, 2200−2206.
(17) Aqil, F.; Munagala, R.; Jeyabalan, J.; Vadhanam, M. V. Bioavailability of phytochemicals and its enhancement by drug delivery systems. *Cancer Lett.* **2013**, *334*, 133−141.
(18) Wojcikowski, K.; Stevenson, L.; Leach, D.; Wohlmuth, H.; Gobe, G. Antioxidant capacity of 55 medicinal herbs traditionally used to treat the urinary system: a comparison using a sequential three-solvent extraction process. *J. Altern. Complementary Med.* **2007**, *13*, 103−110.
(19) Rajarajeshwari, T.; Shivashri, C.; Rajasekar, P. Synthesis and characterization of biocompatible gymnemic acid−gold nanoparticles: a study on glucose uptake stimulatory effect in 3T3-L1 adipocytes. *RSC Adv.* **2014**, *4*, 63285−63295.
(20) Abbas, O.; Compère, G.; Larondelle, Y.; Pompeu, D.; Rogez, H.; Baeten, V. Phenolic compound explorer: A mid-infrared spectroscopy database. *Vib. Spectrosc.* **2017**, *92*, 111−118.
(21) Kazuko, Y.; Kayoko, A.; Shigenobu, A.; Kouji, M. Gymenmic acids V, VI and VII from Gur-ma, the leaves of Gymnema sylvestre R. *Chem. Pharm. Bull.* **1989**, *37*, 852−854.
(22) Shenoy, R. S.; Prashanth, K. V.; Manonmani, H. K. In vitro antidiabetic effects of isolated triterpene glycoside fraction from Gymnema sylvestre. *J. Evidence-Based Complementary Altern. Med.* **2018**, *2018*, 7154702.
(23) Yoshikawa, K.; Nakagawa, M.; Yamamoto, R.; Arihara, S.; Matsuura, K. Antisweet natural products. V. Structures of gymnemic acids VIII-XII from Gymnema sylvestre R. Br. *Chem. Pharm. Bull.* **1992**, *40*, 1779−1782.
(24) Chen, G.; Guo, M. Rapid screening for α-glucosidase inhibitors from Gymnema sylvestre by affinity ultrafiltration−HPLC-MS. *Front. Pharmacol.* **2017**, *8*, 228−236.
(25) Yoshikawa, M.; Murakami, T.; Matsuda, H. Medicinal foodstuffs. X. Structures of new triterpene glycosides, gymnemosides-c,-d,-e, and-f, from the leaves of Gymnema sylvestre R. BR.: influence of gymnema glycosides on glucose uptake in rat small intestinal fragments. *Chem. Pharm. Bull.* **1997**, *45*, 2034−2038.
(26) Colson, E.; Savarino, P.; Claereboudt, E. J. S.; Cabrera-Barjas, G.; Deleu, M.; Lins, L.; Eeckhaut, I.; Flammang, P.; Gerbaux, P. Enhancing the Membranolytic Activity of Chenopodium quinoa Saponins by Fast Microwave Hydrolysis. *Molecules* **2020**, *25*, 1731.
(27) Behuria, H. G.; Biswal, B. K.; Sahu, S. K. Electroformation of liposomes and phytosomes using copper electrode. *J. Liposome Res.* **2021**, *31*, 255−266.
(28) Hughes, G. W.; Sridhar, P.; Nestorow, S. A.; Wotherspoon, P. J.; Cooper, B. F.; Knowles, T. J. MlaFEDB displays flippase activity to promote phospholipid transport towards the outer membrane of Gram-negative bacteria. **2020**, bioRxiv:10.1101/2020.06.06.138008.
(29) Contreras, F.-X.; Sánchez-Magraner, L.; Alonso, A.; Goñi, F. M. Transbilayer (flip-flop) lipid motion and lipid scrambling in membranes. *FEBS Lett.* **2010**, *584*, 1779−1786.
(30) Inokuchi, T.; Arai, N. Relationship between water permeation and flip-flop motion in a bilayer membrane. *Phys. Chem. Chem. Phys.* **2018**, *20*, 28155−28161.
(31) Reggio, P. H. GPCRs Moonlighting as Scramblases: Mechanism Revealed. *Structure* **2018**, *26*, 184−186.
(32) Razzokov, J.; Yusupov, M.; Vanuytsel, S.; Neyts, E. C.; Bogaerts, A. Phosphatidylserine flip-flop induced by oxidation of the plasma membrane: a better insight by atomic scale modeling. *Plasma Processes Polym.* **2017**, *14*, 1700013−1700020.
(33) Rojewska, M.; Smułek, W.; Prochaska, K.; Kaczorek, E. Combined Effect of Nitrofurantoin and Plant Surfactant on Bacteria Phospholipid Membrane. *Molecules* **2020**, *25*, 2527−2537.
(34) Menon, I.; Huber, T.; Sanyal, S.; Banerjee, S.; Barré, P.; Canis, S.; Warren, J. D.; Hwa, J.; Sakmar, T. P.; Menon, A. K. Opsin is a phospholipid flippase. *Curr. Biol.* **2011**, *21*, 149−153.
(35) Wilhelm, M. J.; Sharifian Gh, M.; Dai, H.-L. Influence of molecular structure on passive membrane transport: A case study by second harmonic light scattering. *J. Chem. Phys.* **2019**, *150*, 104705−104731.
(36) Li, N.; Luo, M.; Fu, Y.-j.; Zu, Y.-g.; Wang, W.; Zhang, L.; Yao, L.-p.; Zhao, C.-j.; Sun, Y. Effect of corilagin on membrane permeability of Escherichia coli, Staphylococcus aureus and Candida albicans. *Phytother. Res.* **2013**, *27*, 1517−1523.
(37) Guo, N.; Gai, Q.-Y.; Jiao, J.; Wang, W.; Zu, Y.-G.; Fu, Y.-J. Antibacterial activity of Fructus forsythia essential oil and the application of EO-loaded nanoparticles to food-borne pathogens. *Foods* **2016**, *5*, 73−82.
(38) Lopez-Romero, J. C.; González-Ríos, H.; Borges, A.; Simões, M. Antibacterial effects and mode of action of selected essential oils components against Escherichia coli and Staphylococcus aureus. *Evidence-Based Complementary Altern. Med.* **2015**, *2015*, 795435.
(39) Zhang, J.; Ye, K.-P.; Zhang, X.; Pan, D.-D.; Sun, Y.-Y.; Cao, J.-X. Antibacterial activity and mechanism of action of black pepper essential oil on meat-borne Escherichia coli. *Front. Microbiol.* **2017**, *7*, 2094−2103.
(40) Trombetta, D.; Castelli, F.; Sarpietro, M. G.; Venuti, V.; Cristani, M.; Daniele, C.; Saija, A.; Mazzanti, G.; Bisignano, G. Mechanisms of antibacterial action of three monoterpenes. *Antimicrob. Agents Chemother.* **2005**, *49*, 2474−2478.
(41) Ingólfsson, H. I.; Thakur, P.; Herold, K. F.; Hobart, E. A.; Ramsey, N. B.; Periole, X.; De Jong, D. H.; Zwama, M.; Yilmaz, D.; Hall, K.; Maretzky, T.; Hemmings, H. C.; Blobel, C.; Marrink, S. J.; Koçer, A.; Sack, J. T.; Andersen, O. S. Phytochemicals perturb membranes and promiscuously alter protein function. *ACS Chem. Biol.* **2014**, *9*, 1788−1798.
(42) Peterson, B.; Weyers, M.; Steenekamp, J.; Steyn, J.; Gouws, C.; Hamman, J. Drug bioavailability enhancing agents of natural origin (bioenhancers) that modulate drug membrane permeation and pre-systemic metabolism. *Pharmaceutics* **2019**, *11*, 33.
(43) Veras, H. N. H.; Rodrigues, F. F. G.; Botelho, M. A.; Menezes, I. R. A.; Coutinho, H. D. M.; Costa, J. G. M. Enhancement of aminoglycosides and β-lactams antibiotic activity by essential oil of Lippia sidoides Cham.;the thymol. *Arabian J. Chem.* **2017**, *10*, S2790−S2795.
(44) Farrag, H. A.; Abdallah, N.; Shehata, M. M. K.; Awad, E. M. Natural outer membrane permeabilizers boost antibiotic action against irradiated resistant bacteria. *J. Biomed. Sci.* **2019**, *26*, 69.
(45) Sahu, S. K.; Gummadi, S. N. Flippase activity in proteoliposomes reconstituted with Spinacea oleracea endoplasmic reticulum membrane proteins: evidence of biogenic membrane flippase in plants. *Biochemistry* **2008**, *47*, 10481−10490.
(46) Blicharski, T.; Oniszczuk, A. Extraction methods for the isolation of isoflavonoids from plant material. *Open Chem.* **2017**, *15*, 34−45.
(47) Ejikeme, C.; Ezeonu, C. S.; Eboatu, A. N. Determination of Physical and Phytochemical Constituents of some Tropical Timbers Indigenous to nigerdelta area of Nigeria. *Eur. Sci. J.* **2014**, *10*, 247−270.
(48) Pathan, R. A.; Bhandari, U. Gymnemic acid-phospholipid complex: preparation and characterization. *J. Dispersion Sci. Technol.* **2011**, *32*, 1165−1172.
(49) Bakari, S.; Hajlaoui, H.; Daoud, A.; Mighri, H.; Ross-Garcia, J. M.; Gharsallah, N.; Kadri, A. Phytochemicals, antioxidant and antimicrobial potentials and LC-MS analysis of hydroalcoholic extracts of leaves and flowers of Erodium glaucophyllum collected from Tunisian Sahara. *Food Sci. Technol.* **2018**, *38*, 310−317.

https://doi.org/10.1021/acsomega.1c05581
ACS Omega 2021, 6, 35667−35678

(50) Ansari, M. A.; Fatima, Z.; Hameed, S. Anticandidal effect and mechanisms of monoterpenoid, perillyl alcohol against Candida albicans. *PLoS One* **2016**, *11*, No. e0162465.
(51) Devi, K. P.; Nisha, S. A.; Sakthivel, R.; Pandian, S. K. Eugenol (an essential oil of clove) acts as an antibacterial agent against Salmonella typhi by disrupting the cellular membrane. *J. Ethnopharmacol.* **2010**, *130*, 107−115.
(52) Diao, W.-R.; Hu, Q.-P.; Zhang, H.; Xu, J.-G. Chemical composition, antibacterial activity and mechanism of action of essential oil from seeds of fennel (Foeniculum vulgare Mill.). *Food Control* **2014**, *35*, 109−116.
(53) Fiske, C. H.; Subbarow, Y. The colorimetric determination of phosphorus. *J. Biol. Chem.* **1925**, *66*, 375−400.
(54) Khan, I.; Bahuguna, A.; Kumar, P.; Bajpai, V. K.; Kang, S. C. Antimicrobial potential of carvacrol against uropathogenic Escherichia coli via membrane disruption, depolarization, and reactive oxygen species generation. *Front. Microbiol.* **2017**, *8*, 2421.
(55) Yang, Z.-G.; Sun, H.-X.; Fang, W.-H. Haemolytic activities and adjuvant effect of Astragalus membranaceus saponins (AMS) on the immune responses to ovalbumin in mice. *Vaccine* **2005**, *23*, 5196−5203.
(56) Mun, S.-H.; Joung, D.-K.; Kim, Y.-S.; Kang, O.-H.; Kim, S.-B.; Seo, Y.-S.; Kim, Y.-C.; Lee, D.-S.; Shin, D.-W.; Kweon, K.-T.; Kwon, D.-Y. Synergistic antibacterial effect of curcumin against methicillin-resistant Staphylococcus aureus. *Phytomedicine* **2013**, *20*, 714−718.

https://doi.org/10.1021/acsomega.1c05581
ACS Omega 2021, 6, 35667−35678